ISSN 1392–1320 MATERIALS SCIENCE (MEDŽIAGOTYRA). Vol. 19, No. 3. 2013

Kinetics of Ni:C Thin Film Composition Formation at Different Temperatures and Fluxes

Gediminas KAIRAITIS *, Arvaidas GALDIKAS

Physics Department, Kaunas University of Technology, 50 Studentų st., LT-51368 Kaunas, Lithuania

crossref http://dx.doi.org/10.5755/j01.ms.19.3.5234

Received 17 February 2012; accepted 15 December 2012

In this work analysis considering Ni:C thin films growth on thermaly oxidized Si substrate by proposed kinetic model is presented. Model is built considering experimental results where microstructure evolution as a function of the substrate temperature and metal content of Ni:C nanocomposite films grown by hyperthermal ion deposition is investigated. The proposed kinetic model is based on the rate equations and includes processes of adsorption, surface segregation, diffusion, chemical reactions of constituents. The experimental depth profile curves were fitted by using proposed model. The obtained results show a good agreement with experiment taking into account concentration dependent diffusion. It is shown by modeling that with the increase of substrate temperature the process of nickel surface segregation becomes most important.

Keywords: modeling, kinetics, diffusion, segregation, thin films.

1. INTRODUCTION

Multiphase nanostructured thin films have attracted a significant attention in the last two decades due to their multifunctionality [1]. These structures are two or multicomponent systems containing additives of varying concentration beside the film material. Carbon-based composite thin films have large application potential because of their unique mechanical properties, high hardness, high elasticity, and a low widely adjustable friction coefficient [2]. Carbon films are alternatively modified by the addition of metals, e. g. Ni, Cu, Ag, and Cr, etc [2]. Nanoscaled thin metallic films are of great importance in scientific and technological fields, including microelectronics, optical devices, catalysis, and chemical and biological sensors, nanocomposite thin films consisting of hard constituents can exhibit mechanical properties that are critical to magnetic storage devices, cutting tools, etc. [3]. Numerous metallic elements have been reported to be encapsulated in carbon cages [4 – 8]. In this case the grains of nanocomposite thin film are surrounded and separated by carbon phase. In general the grain size of the film material decreases with increasing concentration of encapsulating media and can be as low as 1 nm – 10 nm [9]. These encapsulated structures can be obtained by various methods such as arc evaporation [7, 10], plasma enhanced chemical vapor deposition [11] or sputtering [5, 12]. Similar structures obtained after thin film growth using different transitions metals [13] as well as different encapsulating media (carbon, CN_x [8]) suggest that there are common mechanisms which govern the formation of these structures [4].

Mechanical, electrical properties of Ni:C correlate with their nanostructure, this could be of some importance for development of technology, so it is important to control growth morphologies [2, 14]. The nanostructure can be controlled by process parameters such as substrate temperature, incident ion energy and flux, etc. The following growth processes controlling nanostructural evolution: nucleation, island growth, impingement and coalescence of islands, grain coarsening, formation of polycrystalline islands and channels, development of a continuous structure, and film growth [1].

In this work analysis of Ni:C thin films growth on oxidized Si substrate by proposed kinetic model is presented. The proposed kinetic model is based on the rate equations and includes such processes as adsorption, surface segregation, diffusion, chemical reactions of constituents. The experimental depth profile curves from ref. [6] were fitted by using proposed model. The obtained modelling results are in good agreement with the experimental depth profiles, from which the conclusions about film growth mechanisms and kinetics are done.

2. KINETIC MODEL

Considering experimental results [6] presented in Figs. 1 – 5 (dotted curves) where composition depth profiles of Ni:C films grown at different substrate temperatures (Figs. 1 – 3) and different contents of Ni (Figs. 2, 4, 5) are presented, it can be seen that at low substrate temperatures (300 °C or 20 °C) the Ni distribution is homogeneous over the whole film. Further increase in the substrate temperature up to 500 °C results to the increase of Ni atomic ratio near the surface. G. Abrasonis and co-workers [6] proposed that increase in the substrate temperature activates process of nickel surface segregation. Also, according to ref. [6] the presence of nickel carbide is observed at substrate temperatures of 300 °C or 20 °C. So the following components are considered in the model

*Corresponding author: ph.: +370-612-47469; fax: +370-37-456472.
E-mail: *gediminas.kairaitis@stud.ktu.lt* (G. Kairaitis)

SiO_2, C, Ni, Ni_3C concentrations in the i-th monolayer are denoted as $c_{SiO_2}^{(i)}, c_C^{(i)}, c_{Ni}^{(i)}, c_{N_3C}^{(i)}, i = \overline{1,N}$, respectively.

Taking into account proposals from G. Abrasonis and co-workers [6], the following processes are included in the model: adsorption of carbon and nickel, diffusion, surface segregation of nickel, formation of nickel carbide compounds and its decomposition.

Adsorption rate is defined following: $V_a = k_{21}c_{SiO_2}^{(1)}i_C + k_{22}c_C^{(1)}i_C + k_{23}c_{Ni}^{(1)}i_C + k_{24}c_{Ni_3C}^{(1)}i_C + k_{31}c_{SiO_2}^{(1)}i_{Ni} + k_{32}c_C^{(1)}i_{Ni} + k_{33}c_{Ni}^{(1)}i_{Ni} + k_{34}c_{Ni_3C}^{(1)}i_{Ni}$, where k_{lp} are the sticking coefficients of *l*-th atoms to the *p*-th component, where $i_C(i_{Ni})$ is the carbon(nickel) ions flux density, where $c_A^{(1)}$ is the relative concentration of the component A on the surface. Natural numbers are related with the constituent components as follows: 1 – SiO_2; 2 – C; 3 – Ni; 4 – Ni_3C. Therefore, *l* = 2, 3 and *p* = 1, 2, 3, 4. The changes of relative concentration of constituent component due to adsorption can be expressed

$$\begin{cases} \left(\frac{dc_{SiO_2}^{(1)}}{dt}\right)_{Ad} = -k_{21}c_{SiO_2}^{(1)}i_C^0 - k_{31}c_{SiO_2}^{(1)}i_{Ni}^0 \\ \left(\frac{dc_C^{(1)}}{dt}\right)_{Ad} = k_{21}c_{SiO_2}^{(1)}i_C^0 + k_{23}c_{Ni}^{(1)}i_C^0 + k_{24}c_{Ni_3C}^{(1)}i_C^0 - k_{32}c_C^{(1)}i_{Ni}^0 \\ \left(\frac{dc_{Ni}^{(1)}}{dt}\right)_{Ad} = k_{31}c_{SiO_2}^{(1)}i_{Ni}^0 + k_{32}c_C^{(1)}i_{Ni}^0 + k_{34}c_{Ni_3C}^{(1)}i_{Ni}^0 - k_{23}c_{Ni}^{(1)}i_C^0 \\ \left(\frac{dc_A^{(i)}}{dt}\right)_{Ad} = \frac{V_a(c_A^{(i-1)} - c_A^{(i)})}{m}, \\ A \in \{SiO_2, C, Ni, Ni_3C\}, i = \overline{2,N}, \end{cases} \quad (1)$$

where: $i_{Ni}^0 = i_{Ni}/m; i_C^0 = i_C/m$, the term $V_a(c_A^{(i-1)} - c_A^{(i)})$ means that after adsorption on the surface component A of $i-1$-th monolayer moves to a deeper monolayer, where $m = h/2.3\cdot10^{-10}$, *h* is the thickness of one layer in meters, $2.3\cdot10^{-10}$ is the thickness of one monolayer in meters.

The process of diffusion is defined using Fick's second law expressed in finite increments

$$\begin{cases} \left(\frac{dc_A^{(1)}}{dt}\right)_{Dif} = d_A(c_A^{(2)} - c_A^{(1)}) \\ \left(\frac{dc_A^{(i)}}{dt}\right)_{Dif} = d_A(c_A^{(i+1)} - 2c_A^{(i)} + c_A^{(i-1)}) \\ \left(\frac{dc_A^{(N)}}{dt}\right)_{Dif} = d_A(c_A^{(N-1)} - c_A^{(N)}) \\ A \in \{SiO_2, C, Ni\}, i = \overline{2,N-1} \end{cases}, \quad (2)$$

where $d_A = D_A/h^2$, D_A is the diffusion coefficient of component A and *h* is the thickness of one layer.

It is assumed that the flux of nickel to *i*-th layer due to surface segregation is directly proportional to relative nickel concentration in deeper $i+1$-th layer:

$$\begin{cases} \left(\frac{dc_{Ni}^{(1)}}{dt}\right)_{Seg} = Sc_{Ni}^{(2)} \\ \left(\frac{dc_{Ni}^{(i)}}{dt}\right)_{Seg} = Sc_{Ni}^{(i+1)} - Sc_{Ni}^{(i)}, i = \overline{2,N-1} \\ \left(\frac{dc_{Ni}^{(N)}}{dt}\right)_{Seg} = -Sc_{Ni}^{(N)} \\ \left(\frac{dc_C^{(i)}}{dt}\right)_{Seg} = -\left(dc_{Ni}^{(i)}/dt\right)_{Seg}, i = \overline{1,N} \end{cases}, \quad (3)$$

where S is the surface segregation coefficient.

The formation rate of Ni_3C compound is defined using the equation of chemical kinetics (mass action law):

$$\begin{cases} \left(\frac{dc_C^{(i)}}{dt}\right)_F = -\frac{1}{4}k_1(c_{Ni}^{(i)})^3c_C^{(i)} \\ \left(\frac{dc_{Ni}^{(i)}}{dt}\right)_F = -\frac{3}{4}k_1(c_{Ni}^{(i)})^3c_C^{(i)} \\ \left(\frac{dc_{Ni_3C}^{(i)}}{dt}\right)_F = k_1(c_{Ni}^{(i)})^3c_C^{(i)}, \\ i = \overline{1,N} \end{cases}, \quad (4)$$

where $k_1 = A_1 e^{-\frac{E_1}{k_B T}}$ is the reaction rate constant, where E_1 is the activation energy of the process.

The decomposition rate of nickel carbide compound is expressed

$$\begin{cases} \left(\frac{dc_C^{(i)}}{dt}\right)_D = \frac{1}{4}k_2c_{Ni_3C}^{(i)} \\ \left(\frac{dc_{Ni}^{(i)}}{dt}\right)_D = \frac{3}{4}k_2c_{Ni_3C}^{(i)} \\ \left(\frac{dc_{Ni_3C}^{(i)}}{dt}\right)_D = -k_2c_{Ni_3C}^{(i)}, \\ i = \overline{1,N} \end{cases}, \quad (5)$$

where $k_2 = A_2 e^{-\frac{E_2}{k_B T}}$ is the reaction rate constant.

Including all the processes described above the system of equations takes following form:

$$\begin{cases} \frac{dc_{SiO_2}^{(i)}}{dt} = \left(\frac{dc_{SiO_2}^{(i)}}{dt}\right)_{Ad} + \left(\frac{dc_{SiO_2}^{(i)}}{dt}\right)_{Dif} \\ \frac{dc_{Ni_3C}^{(i)}}{dt} = \left(\frac{dc_{Ni_3C}^{(i)}}{dt}\right)_{Ad} + \left(\frac{dc_{Ni_3C}^{(i)}}{dt}\right)_F + \left(\frac{dc_{Ni_3C}^{(i)}}{dt}\right)_D. \\ \frac{dc_A^{(i)}}{dt} = \left(\frac{dc_A^{(i)}}{dt}\right)_{Ad} + \left(\frac{dc_A^{(i)}}{dt}\right)_{Dif} + \left(\frac{dc_A^{(i)}}{dt}\right)_{Seg} \\ + \left(\frac{dc_A^{(i)}}{dt}\right)_F + \left(\frac{dc_A^{(i)}}{dt}\right)_D, A \in \{C, Ni\}, i = \overline{1,N} \end{cases} \quad (6)$$

3. RESULTS AND DISCUSSION

The experimental depth profile curves from refs. [6] were fitted by using the proposed model. In these experiments Ni:C nanocomposite thin films were deposited by pulsed filtered cathodic vacuum arc on thermally oxidized Si substrates. Films were deposited with the substrate temperature varied in the range from room temperature (RT) to 500 °C and with the Ni content ranging from 7 at.% to 30 at.%. The elemental depth profiles and composition were determined by elastic recoil detection analysis.

To calculate elemental profiles equations (6) were solved numerically. The model involves diffusion of all components except Ni_3C due to concentration gradient. For segregation it is assumed that the changes of nickel relative concentration due to surface segregation are accompanied by opposite changes of relative carbon concentration. The following coefficients are undefined parameter and in this work was extracted by fitting the experimental curves of depth profiles: three diffusion coefficients (D_{Ni}), (D_C), ($D_{Si:O}$), the nickel surface segregation coefficient (S) and all the sticking coefficients. All other parameters were defined from experiment. The calculations are started from the following initial composition: $c^{(i)}_{SiO_2} = 1, c^{(i)}_{C} = 0, c^{(i)}_{Ni} = 0, c^{(i)}_{Ni_3C} = 0, i = \overline{1, N}$. The values of parameters obtained from the fits are presented in Table 1 and Table 3.

Table 1. Values of parameters obtained by fitting of experimental results at T = 500 °C

	T = 500 °C		
	Ni content of 7 at.%	Ni content of 15 at.%	Ni content of 30 at.%
k_{22}	0.95		
k_{23}	1		
k_{32}	0.8		
k_{33}	0.9		
S, s^{-1}	308		
D_{Ni}, m^2/s	$3.48 \cdot 10^{-15}$	$2.08 \cdot 10^{-15}$	$1.25 \cdot 10^{-15}$
D_C, m^2/s	$3.78 \cdot 10^{-18}$	$6.1 \cdot 10^{-17}$	$1.89 \cdot 10^{-16}$
$D_{Si:O}$, m^2/s	$3.78 \cdot 10^{-18}$	$6.1 \cdot 10^{-17}$	$1.89 \cdot 10^{-16}$
N	940	1080	1184
i_{Ni}, s^{-1}	28.2	56.4	112.8

All the other parameters are kept constant. Values of the others parameters are presented in Table 2.

Table 2. Values of the constant parameters

k_{21}	k_{31}	k_{24}	k_{34}	h, m	i_C, s^{-1}
0.5	0.25	0.8	0.45	$2.3 \cdot 10^{-10}$	282

Fitting results of the depth profiles are presented in Figs. 1 – 5 (solid lines) together with the experimental points [6]. Fittings are done at different flux of nickel (Figs. 1 – 3) and at different temperatures of substrates (Figs. 2, 4, 5). Fittings are done for all constituent components. All calculated curves for all cases and for all the constituent components show good agreement with the experimental results indicating validity of the model.

Table 3. Values of parameters obtained by fitting of experimental results at T = 20 °C and at T = 300 °C

	T = 20 °C	T = 300 °C
	Ni content of 15 at.%	Ni content of 15 at.%
k_{22}	0.8	
k_{23}	1	
k_{32}	0.63	0.9
k_{33}	0.9	
S, s^{-1}	<30	
D_{Ni}, D_C, $D_{Si:O}$, m^2/s	$7.62 \cdot 10^{-18}$	$2.28 \cdot 10^{-17}$
N	768	1024
i_{Ni}, s^{-1}	56.4	

From Figs. 1 – 3 it can be seen that at temperature of 500 °C experimental atomic concentration of nickel is higher at the surface and exponentially decreases with depth while at low temperatures 300 °C and RT the profile of Ni concentration is horizontal (Figs. 4, 5). It is important to note that such increasing of Ni atomic ratio at the surface is obtained during modeling by including process of surface segregation of Ni (eq. (3)). When the surface segregation of nickel is relatively low only homogeneous depth profile curves of Ni (see Figs. 4, 5) can be obtained. It should be noted that an extension of eq. (3) is used to model surface segregation in various binary systems such as Ni:Cu, Ag:Cu [17, 18].

According to the experimental results surface segregation of Ni is negligible at temperature of 300 °C or less. It is shown by modeling that at such temperatures surface segregation coefficient of nickel is at least order of magnitude lower compared with segregation coefficient at temperature of 500 °C (Table 3).

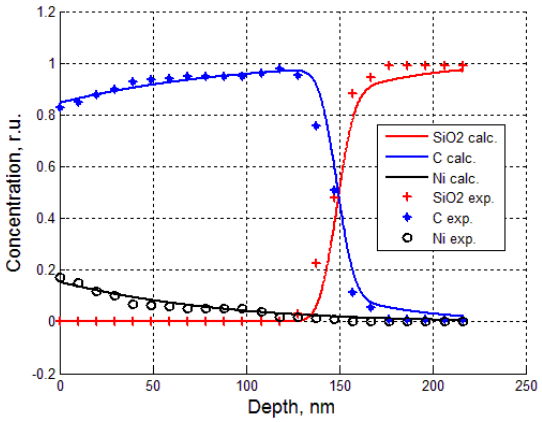

Fig. 1. Experimental [6] (points) and calculated (lines) depth profiles of components at 500 °C with Ni content of 7 at.%

The reaction rate constants k_1, k_2 are expressed by Arrhenius law and depend on temperature. Ni_3C compound is metastable and decomposes into its components at higher

temperatures than 300 °C. So, the rate constants k_1, k_2 are such that at lower temperatures (300 °C or 20 °C) formation of Ni_3C prevails over decomposition and at higher growth temperature decomposition of Ni_3C prevails over formation. At temperature of 500 °C Ni_3C concentration is close to zero and elemental nickel can segregate (eq. (3)) to the surface.

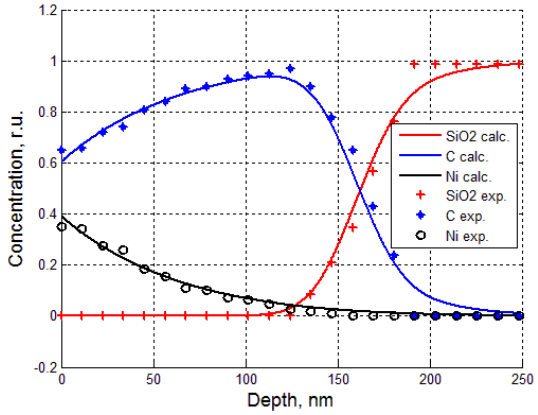

Fig. 2. Experimental [6] (points) and calculated (lines) depth profiles of components at 500 °C with Ni content of 15 at.%

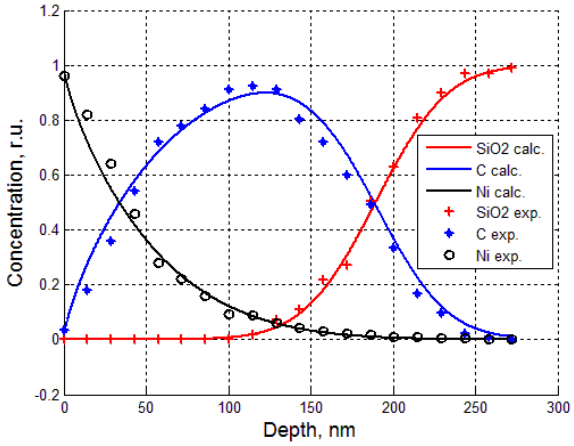

Fig. 3. Experimental [6] (points) and calculated (lines) depth profiles of components at 500 °C with Ni content of 30 at.%

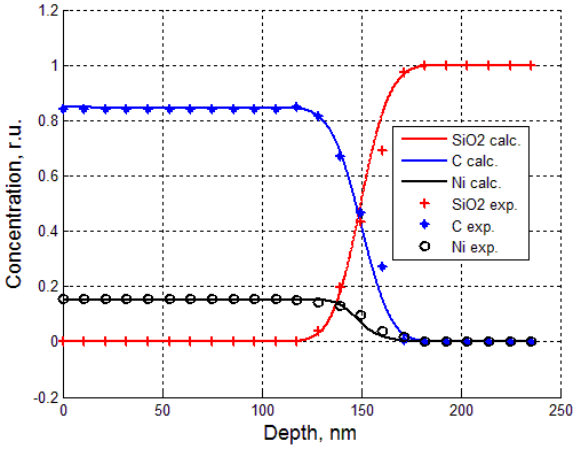

Fig. 4. Experimental [6] (points) and calculated (lines) depth profiles of components at 300 °C with Ni content of 15 at.%

It was found by fitting of experimental points at 500 °C and at different Ni fluxes that diffusion coefficient depends on Ni concentration according to well-known Einstein-Smoluchowski relation $D_{Ni} \sim 1/c_{Ni}$ [15, 16]. The found values of diffusion coefficient versus $1/c_{Ni}$ are plotted in Fig. 6 which show linear dependence (R^2 value near to 1). The same relation between diffusion coefficient and concentration was obtained in some other works [19]. Also, from Table 1 it can be seen that diffusion coefficients D_C, $D_{Si:O}$, increases with increasing flux of nickel ions, so $D_C, D_{Si:O} \sim i_{Ni}$. Dependence of diffusion coefficient on incoming particle flux is characteristic for radiation-enhanced diffusion. Hence, radiation-enhanced diffusion is observed in this case. It is important to note that diffusion coefficient of nickel decreases with increasing flux of nickel ions because $D_{Ni} \sim 1/c_{Ni}$ and $i_{Ni} \sim c_{Ni}$.

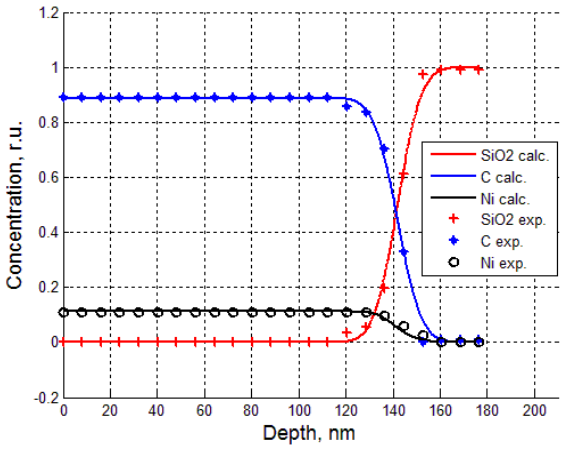

Fig. 5. Experimental [6] (points) and calculated (lines) depth profiles of components at room temperature with Ni content of 15 at.%

From Fig. 1 it can be seen that for the Ni:C film grown at low Ni flux, experimental Ni concentration profile exhibits a weakly observed plateau of ~5 at.% at a depth of ~50 nm – 100 nm, but calculated Ni profile slowly varies at such depth. Near the surface both experimental and calculated Ni atomic ratios increase to a maximum of ~16 at.%. For the higher Ni fluxes (Figs. 2, 3) such a plateau is not observed and calculated depth profiles are in good agreement with experimental results. At very high Ni flux (Fig. 3) the Ni:C film consists of the Ni layer of variable thickness on the top of the carbon layers, both experimental and calculated Ni relative concentrations increase to a maximum of ~100 at.% at the surface. In all profiles at 500 °C carbon concentration is lower at the surface and increases with depth, showing that during surface segregation of Ni carbon moves to deeper layers.

At temperatures of 300 °C and RT the depth distribution profiles of nickel and carbon are homogeneous within the film. At temperature of 300 °C (Fig. 4) experimental and calculated Ni depth profiles exhibit a plateau of ~(15 – 16) at.% within the film. At room temperature (Fig. 5) experimental and calculated Ni depth profiles exhibit a plateau of ~10 at.% within the film. The surface segregation of Ni is negligible process at those temperatures. The formation of compounds Ni_3C prevails

and nickel cannot segregate because of its low mobility. The formation of Ni_3C compounds also results in homogeneous distribution of Ni and C over the film.

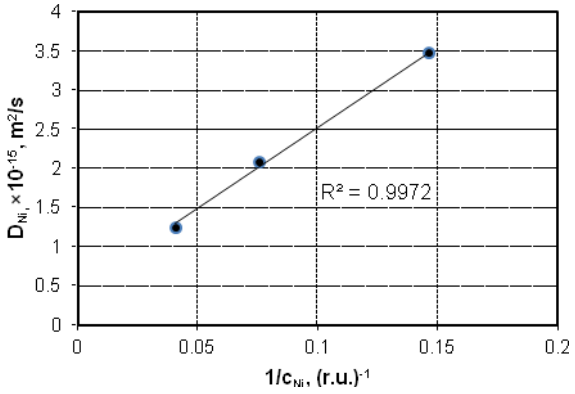

Fig. 6. Dependence of found by fitting values of diffusion coefficients (points) on $1/c_{Ni}$ indicating linear dependence $D_{Ni} \sim 1/c_{Ni}$

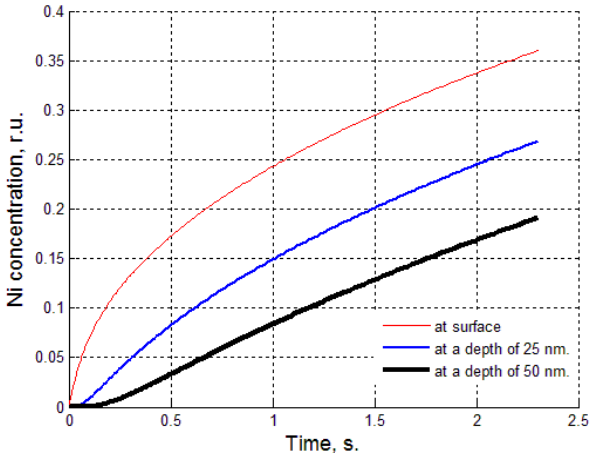

Fig. 7. Plot of relative concentration of Ni versus time at 500 °C with Ni content of ~15 at.%

Considering the growth at different depth from Fig. 8 it can be seen that at low temperature the curves are similar only some delay in deeper layers take place.

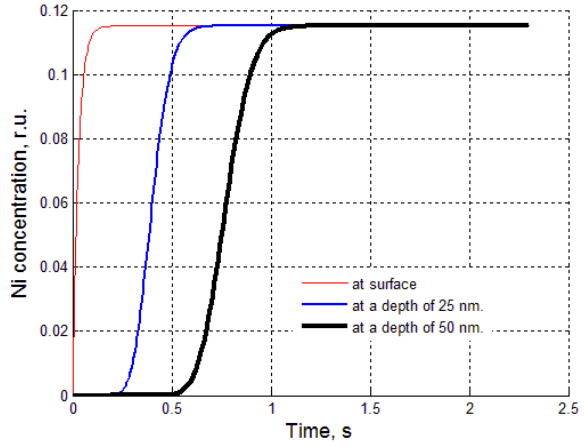

Fig. 8. Plot of relative concentration of Ni versus time at room temperature with Ni content of ~15 at.%

In Figs. 7, 8 the evolution of Ni relative concentration in time of film growth at different depth at high and low temperatures is presented. In the case of low temperatures (Fig. 8) curves very fast approaches the steady state values. At high temperature (Fig. 7) the curves increases slowly. However comparing curves obtained for high and low temperatures it must be taken into account the total amount of Ni at considered depth is quite different. In Fig. 8 steady state value of Ni concentration is at less than 0.12 while in Fig. 7 Ni concentration is much higher and obviously that the time to reach steady state is much higher. Nevertheless, derivative of $\frac{dc_{Ni}^{(1)}}{dt}$ for higher temperatures is more and it is because of segregation process.

At high temperatures as it is seen form Fig. 7 the shapes of curves at different depth are quite different: curve for surface show that the derivative $\frac{dc_{Ni}^{(1)}}{dt}$ is highest at the beginning of process and later decreases. This derivative for curve at depth 50 nm behaves contrarily: is less at the beginning and later increases.

4. CONCLUSIONS

Considering kinetic of Ni:C thin film growth at different temperatures and different Ni fluxes the following conclusions can be stated:

1. At temperatures of 300 °C or less the formation of compounds Ni_3C prevails.
2. At temperatures higher than 300 °C the decomposition of Ni_3C prevails.
3. At temperature of 500 °C the surface segregation of Ni is most important process while at lower temperatures the surface segregation is negligible.
4. Diffusion coefficient of Ni depends on concentration according the $1/c_{Ni}$ law.

REFERENCES

1. **Petrov, I., Barna, P.-B., Hultman, L., Green, J.-E.** Microstructural Evolution during Film Growth *Journal of Vacuum Science & Technology A* 21 (5) 2003: pp. 117 – 128. http://dx.doi.org/10.1116/1.1601610
2. **Sedlacková, K., Lobotka, P., Vávra, I., Radnóczi, G.** Structural, Electrical and Magnetic Properties of Carbon–Nickel Composite Thin Films *Carbon* 43 2005: pp. 2192 – 2198.
3. **Wan-Yu Wu, Chia-Wei Hsu, Jyh-Ming Ting.** Nanoscaled C, Ni, Pt Thin Films *Journal of Nano Research* 6 2009: pp. 29 – 34.
4. **Abrasonis, G., Krause, M., Mücklich, A., Sedlacková, K., Radnóczi, G., Kreissig, U., Kolitsch, A., Möller, W.,** Growth Regimes and Metal Enhanced 6-fold Ring Clustering of Carbon in Carbon–Nickel Composite Thin Films *Carbon* 45 2007: pp. 2995 – 3006.
5. **Babonneau, D., Cabioc'h, T., Naudon, A., Girard, J. C., Denanot, M.-F.** Silver Nanoparticles Encapsulated in Carbon Cages Obtained by Cosputtering of the Metal and Graphite *Surface Science* 409 (2) 1998: pp. 358 – 371.
6. **Abrasonis, G., Kovács, Gy.-J., Ryves, L., Krause, M., Mücklich, A., Munnik, F., Oates, T.-W.-H., Bilek, M.-M.-M., Möller, W.** Phase Separation in Carbon-Nickel Films during Hyperthermal Ion Deposition *Journal of Applied Physics* 105 2009: p. 083518. http://dx.doi.org/10.1063/1.3110187

7. **Oku, T., Kusunose, T., Hirata, T., Hatakeyama, R., Sato, N., Niihara, K.,** Formation and Structure of Ag, Ge and SiC Nanoparticles Encapsulated in Boron Nitride and Carbon Nanocapsules *Diamond and Related Materials* 9 (3–6) 2000: pp. 911 – 915. http://dx.doi.org/10.1016/S0925-9635(99)00214-9
8. **Kovács, G.-J., Sáfrán, G., Geszti, O., Ujvári, T., Bertóti, I., Radnóczi, G.** Structure and Mechanical Properties of Carbon–Nickel and CNx–Nickel Nanocomposite Films *Surface and Coatings Technology* 2004: pp. 180 – 181, 331 – 334.
9. **Barna, P., Adamik, M., Labar, J., Kover, L., Toth, J., Devenyi, A., Manaila, R.,** Formation of Polycrystalline and Microcrystalline Composite Thin Films by Codeposition and Surface Chemical Reaction *Surface and Coatings Technology* , 125 2000: pp. 147 – 150.
10. **Ruoff, R.-S., Lorents, D.-C., Chan, B., Malhotra, R., Subramoney, S.** Singlecrystal Metals Encapsulated in Carbon Nanoparticles *Science* 259 (5093) 1993: pp. 346 – 348.
11. **He, C.-N., Du, X.-W., Ding, J., Shi, C.-S., Li, J.-J., Zhao, N.-Q., et al** Low Temperature CVD Synthesis of Carbon-Encapsulated Magnetic Ni Nanoparticles with a Narrow Distribution of Diameters *Carbon* 44 (11) 2006: pp. 2330 – 2333.
12. **Babonneau, D., Jaouen, M., Denanot, M.-F., Guerin, P., Petroff, F.** Nanostructure and Magnetic Properties of BN-encapsulated Fe(B) and Fe2N Nanoparticles Prepared by Dual Ion-beam Sputtering *Applied Physics Letters* 82 (18) 2003: pp. 3056 – 3058.
13. **Jiao, J., Seraphin, S.** Carbon Encapsulated Nanoparticles of Ni, Co, Cu, and Ti *Journal of Applied Physics* 83 (5) 1998: pp. 2442 – 2448.
14. **Radnoczi, G., Kovacs, G.-J., Safran, G., Sedlačkova, K., Geszti, O., Ujvari, T., et al** Structure and Properties of Carbon Based Nanocomposite Films In: Senkov, O. N., et al, editors. Metallic Materials with High Structural Efficiency. Netherlands, Dordrecht: Kluwer Academic Publisher; 2004: pp. 101 – 112. http://dx.doi.org/10.1007/1-4020-2112-7_9
15. **Zoltowski, P.** Diffusion of Hydrogen in Self-stressed Metals — Transfer Function Spectroscopy Approach *Journal of Electroanalytical Chemistry* 501 2001: pp. 89 – 99. http://dx.doi.org/10.1016/S0022-0728(00)00507-6
16. **Moskaliovienė, T., Galdikas, A.** Stress Induced Nitrogen Diffusion in Nitrided Austenitic Stainless Steel *Materials Science* (*Medžiagotyra*) 17 (1) 2011: pp. 11 – 15.
17. **Wang, J.-Y., du-Plessis, J., Terblans, J.-J., van-Wyk, G.-N.** Kinetics Near the Discontinuous Surface Transition in the Cu(Ag)(111) Binary Segregating System *Surface Science* 423 (1) 1999: pp. 12 – 18. http://dx.doi.org/10.1016/S0039-6028(98)00819-X
18. **Yan, X.-L., Wang, J.-Y.** Size Effects on Surface Segregation in Ni–Cu Alloy Thin Films *Thin Solid Films* 2012. doi. 10.1016/j.tsf.2012.03.061. http://dx.doi.org/10.1016/j.tsf.2012.03.061
19. **Moskaliovienė, T., Galdikas, A.** Stress Induced and Concentration Dependent Diffusion of Nitrogen in Plasma Nitrided Austenitic Stainless Steel *Vacuum* 86 (10) 2012: pp. 1552 – 1557.